2013 American Control Conference (ACC)
Washington, DC, USA, June 17-19, 2013

Balanced Deployment of Multiple Robots Using a Modified Kuramoto Model

Zhihao Xu, Magnus Egerstedt, Greg Droge and Klaus Schilling

Abstract— **In this paper, we study the problem of making multiple agents spread out equidistantly on a circle. The proposed solution is a new Kuramoto-like model for multi-robot coordination, in which the standard sine-terms have been replaced by cosines. This new interaction model enables the balanced deployment of agents on a circle, while only taking into account the local information of each agent's two neighbors on a cycle graph. This means that individual agents do not need to know the (relative) states of all agents nor how many other agents are indeed present in the network. We illustrate the operation of the proposed protocol in simulation as well as extend it to a nonlinear scenario by optimizing over the coupling weights.**

I. Introduction

The topic of multiagent coordination has received considerable attention during the last few decades, drawing inspiration from natural phenomena found in biological, physical and social systems, where agents are observed to behave collectively in order to accomplish certain global tasks. This underlying ambition – to go from local rules to global behaviors – has been reflected in many different facets of multi-robot systems, including formation control of unmanned aerial vehicles (UAVs) [1], [2] and satellites [3], [4]; collective motion control of robots [5], [6], and sensor networks [7], [8].

Certain aspects of the multi-agent coordination problem are, by-now, rather well-understood. A prime example of this is the consensus problem, where significant results have been obtained for achieving agreement, synchronization, and area coverage in networks, based in large part on graph theoretic tools, e.g., [9]. One particular protocol for achieving synchronization is the Kuramoto model [10], [11], which was first developed for coupled phase oscillators in an all-to-all network. A detailed review of this model can be found in [12], and [13] analyzed stability issues for the synchronized nonlinear oscillators based on Kuramoto model, and the conditions on the coupling gain in the model derived in their work was later on improved by [14], where both necessary and sufficient conditions on exponential synchronization of the angular frequencies of all oscillators were provided.

This work is supported by the Elitenetwork of Bavaria through the program "Identification, Optimization and Control with Applications in Modern Technologies".

Zhihao Xu and Klaus Schilling are with the Department of Computer Science VII: Robotics and Telematics, University of Würzburg, Germany. E-Mail: {xu,schi}@informatik.uni-wuerzburg.de. Klaus Schilling is also leader of the Zentrum für Telematik, Würzburg, Germany. Magnus Egerstedt and Greg Droge are with School of Electrical and Computer Engineering, Georgia Institute of Technology, Atlanta, GA, USA. E-Mail: {magnus,gregdroge}@gatech.edu

Extensions from the classical Kuramoto models have been pursued recently, including [15] in which transient stability issues in power networks in relation to the synchronization of non-uniform Kuramoto models were investigated. Multi-robot control designs have also been connected to the Kuramoto models, mainly for heading alignment and heading balance control, e.g., [16].

In this paper, we approach an issue that is highly related to synchronization yet philosophically its polar opposite, namely how to make the agents maximally spread out. Within the context of multi-robot coordination, we propose a new Kuramoto-like model for such "balanced deployments" of agents in a decentralized fashion. Instead of having all agents' states synchronized to the same value, we are able to distribute all agents equally on a circle, and the model requires no knowledge of the total number of agents, which is typically needed in centralized control laws. Also, due to the merits of decentralized control, it is possible to add or remove agents from the network, and the balanced deployment will still be achieved and maintained. We further demonstrate the advantage of the proposed Kuramoto-like model in a simple convoy protection scenario, where the control parameters are chosen through a parameterized optimization method.

An interesting related work on area patrolling can be found in [17], where the authors proposed distributed algorithms for an even number of agents to swing on a circle in a synchronized fashion, so that every agent moves back and forth with the same distance and time interval. It, however, addresses the synchronization issue in a different aspect from ours.

The outline of this paper is as follows: Section II will introduce the traditional Kuramoto model used in coupled oscillators. Section III presents our proposed new Kuramoto-like model used for balanced deployment in multi-robot coordination. Section IV provides two simulations, which demonstrate the usage of this model. In Section V, a nonlinear scenario is further formulated and the results are illustrated through the optimization of the control parameters, while the concluding remarks are discussed in Section VI.

II. Synchronization with Kuramoto Model

The classic Kuramoto model consists of N coupled oscillators, whose dynamics are governed by the following equation:

$$\dot{\psi}_i = \omega_i - \frac{K}{N}\sum_{j=1}^{N}\sin(\psi_i - \psi_j), i = 1, ..., N, \qquad (1)$$

978-1-4799-0178-4/$31.00 ©2013 AACC

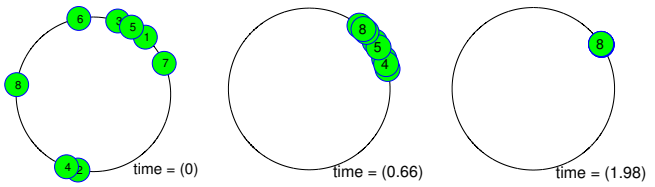

(a) Initial (b) Synchronizing (c) Final

Fig. 1: Phase synchronization example, where $\omega_i = 0$ from Eq. (1)

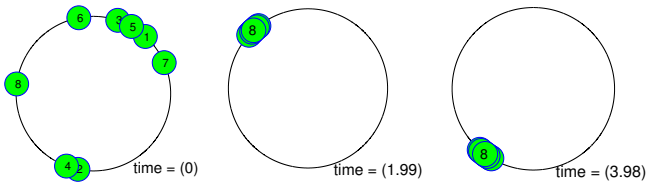

(a) Initial (b) Synchronizing (c) Final

Fig. 2: Frequency synchronization example, where $\omega_i \neq 0$ from Eq. (1)

where ψ_i is the phase of oscillator i, ω_i is the natural frequency, and $K > 0$ is the coupling gain. The oscillators are said to be synchronized if:

$$\lim_{t\to\infty} |\dot{\psi}_i(t) - \dot{\psi}_j(t)| = 0, \forall i, j = 1, ..., N.$$

The necessary condition derived in [14] states that there exists a coupling gain $K = K_c > 0$, below which the oscillators cannot synchronize. Meanwhile, if all the natural frequencies are identical, the phases of the oscillators will converge to a common value ψ_∞, which is referred as *phase synchronization*. If the natural frequencies are non-identical, then each phase difference $\psi_i - \psi_j$ will converge to a constant value, which is not necessarily zero.

As an example of this, consider the results shown in Fig. 1 and Fig. 2, where agents are able to synchronize the phases (positions) and their frequencies (angular velocities) on the circle, respectively.

In the next section, we will extend this Kuramoto model to multi-robot coordination on a cycle graph and propose a new Kuramoto-like model for balanced deployment.

III. New Kuramoto-like model for balanced deployments in cycle graph

A. Graph representation of Kuramoto Model

Consider a cycle graph $\mathcal{G} = (\mathcal{V}, \mathcal{E})$, where $\mathcal{V} = \{\phi_1, ..., \phi_N\}$ denotes the set of nodes, and $\mathcal{E} \subseteq \mathcal{V} \times \mathcal{V}$ is the set of edges. Specifically, $\mathcal{E} = \{(\phi_i, \phi_{i+1})\}, i = 1, ..., N$ and $\phi_0 \triangleq \phi_N, \phi_{N+1} \triangleq \phi_1$. The cardinality of $\mathcal{E}$ is $|\mathcal{E}| = N$. Incidence matrix $D \in \mathbb{R}^{N\times N}$ of a cycle graph is given by [9]:

$$D = \begin{pmatrix} -1 & 0 & \cdots & +1 \\ +1 & -1 & \cdots & 0 \\ \vdots & \ddots & \ddots & \vdots \\ 0 & \cdots & +1 & -1 \end{pmatrix} \tag{2}$$

For such cycle graphs, we have that

$$L = DD^\top = D^\top D = -D - D^\top,$$

where L is the *graph laplacian*. Now we can rewrite the Kuramoto model given in Eq. (1), under the cycle graph topology as follows:

$$\dot{\phi} = \omega - KD\sin(D^\top\phi), \tag{3}$$

where $\phi = [\phi_1, ..., \phi_N]^\top$ are the phases of the oscillators; $\omega = [\omega_1, ..., \omega_N]^\top$; D is given in Eq. (2); $\sin(D^\top\phi) = [\sin(\phi_2 - \phi_1), ..., \sin(\phi_1 - \phi_N)]^\top$.

B. New Kuramoto-like model

Consider a group of N identical vehicles, which have the following dynamics described in polar coordinates:

$$\dot{s} = u, \tag{4}$$

where $s = [\rho, \phi]^\top$ are the positions and orientations of the vehicles, $\rho \in \mathbb{R}^N, \phi \in [0, 2\pi)^N$; $u = [u_1, u_2]^\top$ is the control force, $u_1, u_2 \in \mathbb{R}^N$.

We propose the new Kuramoto-like model for coordinating the orientations of the vehicles as follows:

$$\dot{\phi} = KD\cos(D^\top\phi), \tag{5}$$

where $D \in \mathbb{R}^{N\times N}$ is the incidence matrix; $K > 0$ is the coupling gain; Note that in Eq. (4), we only control the orientation of the vehicle, which means that $u_1 = 0$ in this case.

Theorem 1: In the cycle graph $\mathcal{G}$, assume N vehicles' initial orientations satisfy $0 \leq \phi_1(0) < \phi_2(0) < ... < \phi_N(0) < 2\pi$, $N > 2$, under the dynamics of the new Kuramoto-like model given in Eq. (5), all orientations will asymptotically converge to the balanced distribution on a circle, i.e. $\phi_{i+1} - \phi_i = \frac{2\pi}{N}, \forall i \in \{1, 2, ..., N\}$, where $\phi_{N+1} \triangleq \phi_1$.

Proof: Let $x \triangleq D^\top\phi \mod 2\pi$, which is the orientation difference vector and $x \in [0, 2\pi)^N, \sum_{i=1}^N x_i = 2\pi$. Also, we can calculate:

$$\dot{x} = KD^\top D\cos(x).$$

Consider the following Lyapunov function candidate:

$$V = \frac{1}{2}\|x\|^2 \geq 0 \tag{6}$$

Correspondingly,

$$\begin{aligned} \dot{V} &= x^\top\dot{x} \\ &= Kx^\top D^\top D\cos(x) \\ &= Kx^\top L\cos(x) \\ &= -Kx^\top D\cos(x) - Kx^\top D^\top\cos(x), \end{aligned} \tag{7}$$

where

$$x^\top D\cos(x) = \sum_{i=1}^N (x_{i+1} - x_i)\cos x_i, \quad x_{N+1} \triangleq x_1. \tag{8}$$

According to Proposition 1 in Appendix, we know that $x^\top D\cos(x) \geq 0$ ($x^\top D^\top \cos(x) \geq 0$ can be proved analogously). Therefore, we have $\dot{V} \leq 0$. Now using LaSalle's invariance principle [18], we first define the set $\Omega_c = \{x \in [0, 2\pi)^N | \sum_{i=1}^N x_i = 2\pi, V(x) \leq c, c \in \mathbb{R}^+\}$. Since $\dot{V} \leq 0$ and V is also quadratic, Ω_c is then a compact and positively invariant set. Define

$$V_o = \{x \in \Omega_c | \dot{V} = 0\}. \tag{9}$$

Based on Proposition 1, $\dot{V} = 0 \Leftrightarrow x_{i+1} = x_i, \forall i \in \{1, 2, ..., N\}$. Considering the condition $\sum_{i=1}^N x_i = 2\pi$, we get:

$$V_o = \left\{ x \in \Omega_c | x_i = \frac{2\pi}{N}, \forall i \in \{1, 2, ..., N\} \right\}. \tag{10}$$

Let $M = V_o$, which is (in terms of ϕ):

$$M = \left\{ \phi | \phi_{i+1} - \phi_i = \frac{2\pi}{N} \bmod 2\pi, \forall i \in \{1, 2, ..., N\} \right\}, \tag{11}$$

then every trajectory of ϕ will approach M as $t \to \infty$. This completes the proof. ■

Remarks:

1) The model given in Eq. (5) does not contain ω as in the original Kuramoto model. Therefore, the agents will converge to an equilibrium according to Theorem 1. If we have ω in this model, the agents will spread out to a balanced distribution, while spinning around the circle at a rate of ω.
2) This theorem always holds as long as the initial orientations are not all the same, since the condition of $\sum_{i=1}^N x_i = 2\pi$ does not hold if the initial orientations were the same.
3) From Lemma 2 in Appendix, we see that $\cos(\cdot)$ function can be replaced by some other continuous function that is strictly decreasing on $[0, 2\pi]$, which will still give the same result of $\dot{V} \leq 0$.

IV. Simulation Results

In this section, we will show two simulations, which demonstrate the capability of the new Kuramoto-like model in deploying agents equally on a circle and self-organizing the distribution pattern once new agents are added into the network.

A. Single integrator example

Given $N = 10$ agents with the dynamics of (4) under the network topology of an undirected cycle graph described in Section III. Assume all agents initially line up on a circle of radius $\rho_i = 14, \forall i = 1, 2, ..., N$, and ϕ_i is randomly generated, which is shown in Fig. 3. Using the new Kuramoto-like model described in Eq. (5), we have:

$$u_2 = \dot{\phi} = 10 \cdot D\cos(D^\top \phi), \tag{12}$$

where we set $K = 10$, and incidence matrix D is given in Eq. (2). After 200 simulation steps, these 10 agents end up in a balanced distribution on the circle, as shown in Fig. 4, i.e. $\phi_{i+1} - \phi_i = \frac{2\pi}{10}$. The corresponding Lyapunov function given in Eq. (6) is depicted in Fig. 5.

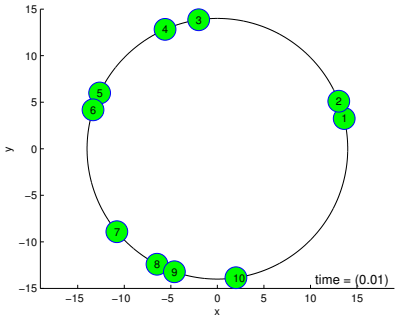

Fig. 3: Initial positions of 10 agents

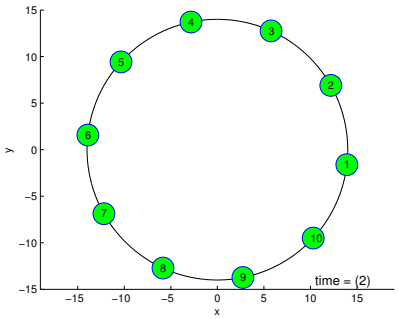

Fig. 4: Final distribution of 10 agents

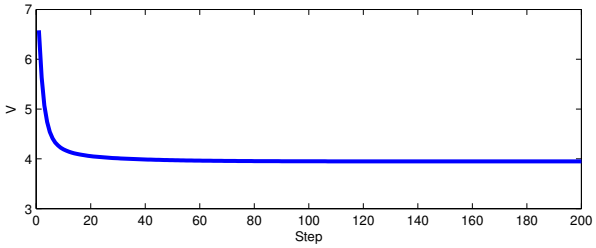

Fig. 5: Lyapunov function of Eq. (6)

B. Self-organizing example

This simulation shows that the positions of agents can be automatically re-organized after adding a number of agents into the network, and still end up with a balanced distribution.

The initial setup of the scene consists of 4 agents on a circle, shown in Fig. 6, which have already settled in a balanced way under Eq. (5). In Fig. 7, 4 more agents are added into the network randomly, where the cycle topology remains. This means the agents can still measure the relative phase difference from their neighbors. And Fig. 8 shows the final distribution of the agents after they reconfigured themselves.

V. Optimal Deployment for Convoy Protection

To show the utility of the new Kuramoto model, we consider the convoy protection scenario given in Fig. 10. In this scenario, we want the agents to follow the movement of the convoy while spreading out along a circular perimeter. To accomplish this task, we will use the new Kuramoto model inside a control-law for a car-like vehicle. As this control law will have tunable gains, we also consider a locker-room agreement where we optimize the gains before deployment depending on the specifics of the scenario. After the initial

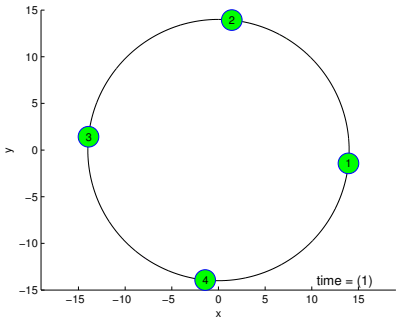

Fig. 6: Initial setup of 4 agents before reconfiguration

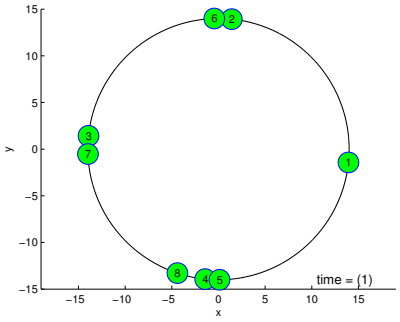

Fig. 7: Agent 5 to 8 added into the network randomly

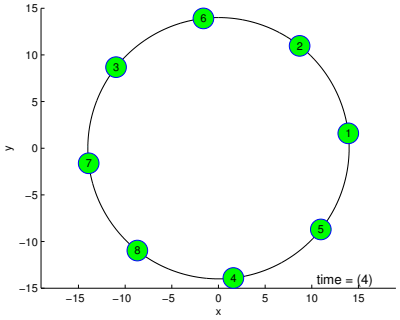

Fig. 8: New distribution after self-reconfiguration

locker room agreement, each agent is able to execute the control law using only information about its neighbors it is connected to through the network. We will end this section with examples showing the optimization giving desirable gains for the convoy protection in two different scenarios.

A. Balanced Convoy Protection

Consider the vehicle in the convoy protection scenario as a standard rear-wheel drive, front-wheel steerable car-like mobile robot (see Fig. 9), whose kinematic equation is given by:

$$\begin{bmatrix} \dot{x}_i(t) \\ \dot{y}_i(t) \\ \dot{\theta}_i(t) \end{bmatrix} = \begin{bmatrix} \cos\theta_i(t) \\ \sin\theta_i(t) \\ [\tan\beta_i(t)]/l \end{bmatrix} v_i(t), \tag{13}$$

where v_i is the translational driving speed; β_i is the equivalent steering angle of the front wheels; (x_i, y_i) is the Cartesian coordinate of the robot in global frame, located at the mid-point of the rear-wheel axle, and θ_i is termed as the orientation; l is the distance between front and rear wheel axle. Note that the first two scalar equations represent the nonholonomic constraints of the car-like mobile robot.

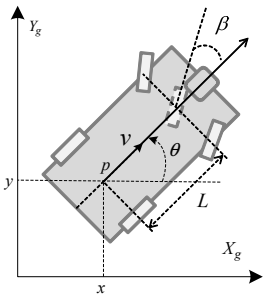

Fig. 9: Model of car-like mobile robot

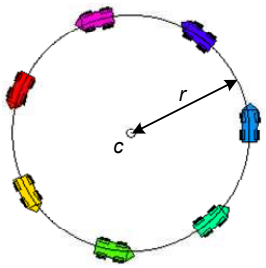

Fig. 10: Convoy protection with car-like robots

Now consider the scenario depicted in Fig. 10 with N vehicles. The collective state q of the system can be given by

$$q = [x^\top, y^\top, \theta^\top, c^\top, r]^\top \in \mathbb{R}^{N\times N\times N\times 2\times 1};$$

$x = [x_1, \ldots, x_N]^\top$, $y = [y_1, \ldots, y_N]^\top$, $\theta = [\theta_1, \ldots, \theta_N]^\top$, c is the coordinate of the central target, and r is the desired radius of the convoy circle, as shown in Fig. 10. The state dynamics are given by[1]:

$$\dot{q} = \begin{bmatrix} \dot{x} \\ \dot{y} \\ \dot{\theta} \\ \dot{c} \\ \dot{r} \end{bmatrix} = \begin{bmatrix} v * \cos\theta \\ v * \sin\theta \\ v * [\tan\beta]/l \\ f_c(t) \\ f_r(t) \end{bmatrix} \triangleq f(q, u, t), \tag{14}$$

where $f_c(t)$ and $f_r(t)$ are the functions describing the motion of the target and the change in convoy radius, respectively, which can be assumed to be given *a prior*. To control the robots to the desired orbit while spreading out, we allow the velocity controls $v \triangleq [v_1, \ldots v_N]^\top$ and steering controls $\beta \triangleq [\beta_1, \ldots \beta_N]^\top$ to be:

$$\begin{cases} v = \omega * d & \text{(15a)} \\ \beta = \arctan\left(\mathbf{1}\dfrac{l}{r} + k_p e + k_d \dot{e}\right) & \text{(15b)} \end{cases}$$

where we incorporate the new Kuramoto model through the angular velocity[2]

$$\omega = u + KD\cos(D^\top\theta) \tag{16}$$

and $e = d - \mathbf{1}r$, $d = \|p - \mathbf{1}c\|^r, p = [p_1, \ldots, p_N]^\top, p_i = [x_i, y_i]^\top, u = [u_1, \ldots, u_N]^\top, e = [e_1, \ldots, e_N]^\top, i = 1, 2, \ldots, N$. We also note that we can express the time

[1]operator $*$ indicates element-wise multiplication.
[2]operator $\|\cdot\|^r$ indicates row-wise norm.

derivative of the error e_i as:

$$\begin{aligned}\frac{de_i}{dt} &= \frac{d\|p_i - c\|}{dt} - f_r(t) \\ &= \frac{(p_i - c)^\top}{\|p_i - c\|}(\dot{p}_i - f_c(t)) - f_r(t) \\ &= \frac{(p_i - c)^\top}{d_i}\begin{pmatrix} v_i\cos\theta_i - f_{c1}(t) \\ v_i\sin\theta_i - f_{c2}(t)\end{pmatrix} - f_r(t) \end{aligned} \quad (17)$$

B. Parameterized Optimal Control

Given the control law outlined above, we must now assign values to the tunable gains. The gains we must assign are k_p and k_d from (15b) as well as the Kuramoto gain K and base angular velocity u from (16). In assigning gains, different aspects must be taken into account. For example, we desire u to be as small as possible in order to expend as little energy as possible while spreading out. However, if the base angular velocity is too small, the vehicles will not travel fast enough to keep up with the moving center. Moreover, different values for u will require different values for k_p, k_d, and K to change the transient response of the system to avoid undesired oscillations.

Optimal control is a technique admissible for this gain tuning as it uses a dynamic model of the system to choose an optimal control action based on some pre-defined cost, [19]. Moreover, we have parameterized control laws as a base for state trajectory generation which can significantly reduce the required computation, [20], [21]. We first consider the general case for parameterized optimal control and then identify costs which will be useful for our purposes.

Parameterized optimal control with corresponding optimality conditions is covered in [21], but we present it here to be complete. Given a system with dynamics

$$\dot{q}(t) = f(q(t), u(t), t), \quad (18)$$

we consider feedback control laws of the form $u(t) = \kappa(q(t), \gamma)$ where γ is a parameter vector. This allows the dynamics to be expressed as

$$\dot{q} = f(q(t), \kappa(q(t), \gamma), t). \quad (19)$$

where we simplify, without loss of generality, as

$$\dot{q} = f(q(t), \gamma, t). \quad (20)$$

In the case of the convoy protection problem, $\kappa(q(t), \gamma)$ is given in (15b) and (16) where $\gamma = \begin{bmatrix} k_d & k_p & K & u\end{bmatrix}^T$.

We now consider a cost to be minimized of the form

$$J(\gamma) = \int_{t_0}^{t_f} L(q(t), \gamma)dt + \Psi(q(t_f), \gamma) \quad (21)$$

subject to (20). In the following theorem we give the first order necessary conditions of optimality which can be used in gradient decent strategies, e.g. [22], to find the optimal set of parameters.

Theorem 2: The first order necessary conditions of optimality for optimizing (21) with respect to the parameter vector, γ, is given by

$$\frac{\partial J}{\partial \gamma} = \xi(t_0) = 0 \quad (22)$$

where

$$\dot{\xi} = -\frac{\partial L}{\partial \gamma}^T - \frac{\partial f}{\partial \gamma}^T \lambda; \xi(t_f) = \frac{\partial \Psi}{\partial \gamma} \quad (23)$$

$$\dot{\lambda} = -\frac{\partial L}{\partial x}^T - \frac{\partial f}{\partial x}^T \lambda; \lambda(t_f) = \frac{\partial \Psi}{\partial x}(x(t_f)). \quad (24)$$

Proof: The proof follows directly from a simplification of the problem considered in [21]. ∎

In the convoy protection problem we are considering, we must balance different objectives. We want the agents to expend as little energy as possible while spreading out, staying on the desired circular orbit, and avoiding oscillations. To spread the agents out and remove undesired oscillations, we define the instantaneous cost as :

$$L(x, \gamma) = L_1(x, \gamma) + L_2(x, \gamma) \quad (25)$$

where

$$L_1(x, \gamma) = \rho_1\big(\cos(\theta_1 - \theta_N) + \sum_{i=2}^{N}\cos(\theta_i - \theta_{i-1})\big) \quad (26)$$

which is designed to spread the agents out and

$$L_2(x, \gamma) = \frac{\rho_2}{2}\sum_{i=1}^{N}(\theta_i - \theta_{id}) \quad (27)$$

where $\theta_{id} = \phi_i + \frac{\pi}{2}$ and $\phi_i = \tan^{-1}(\frac{x_i - c_1}{y_i - c_2})$. This is designed to help reduce undesired oscillations as it keeps the vehicles on a circle.

To ensure that the agents expend as little energy as possible and approach the desired orbit we define the terminal costs as:

$$\Psi(x, \theta) = \Psi_1(x, \theta) + \Psi_2(x, \theta) \quad (28)$$

where

$$\Psi_1(x, \theta) = \frac{\rho_3}{2}\|\omega\|^2 \quad (29)$$

which is designed to have the agents travel as slow as possible and

$$\Psi_2(x, \theta) = \sum_{i=1}^{N}\frac{\rho_4}{2}\|e_i - r\|^2 \quad (30)$$

which is designed to ensure that the agents stabilize on the desired radius.

C. Results

Given the dynamics and optimal control setup, we now illustrate the resulting behavior with two scenarios. Both show the ability of the given control law to spread the agents out. In doing so, they also show the benefit of optimizing over the tunable gains.

The first scenario is shown in Figure 11 which demonstrates the ability of the optimization to adapt the parameters to allow the agents to spread out around the circle while the center is travelling at a rate $f_c(t) = \begin{bmatrix}2 & 2\end{bmatrix}^T$. The optimization finds the optimal gains to be $\begin{bmatrix}k_p & k_d & K & u\end{bmatrix} = \begin{bmatrix}0 & .94 & .39 & 2.79\end{bmatrix}$.

The second scenario is shown in Figure 13 where the center is not moving. The optimization finds the optimal

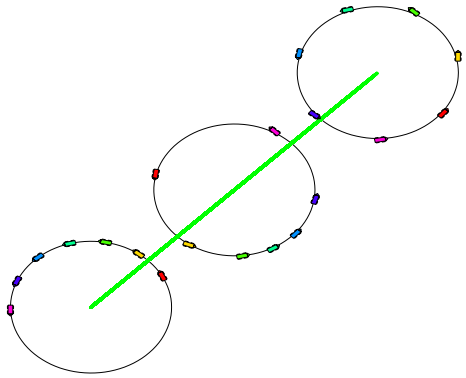

Fig. 11: This figure shows three snapshots of the agents when $f_c = [2 \quad 2]^T$.

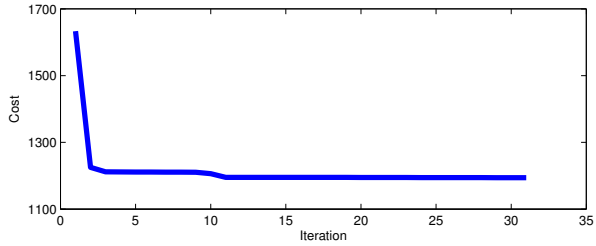

Fig. 12: This figure shows the cost minimization that took place to get the results in Figure 11.

gains to be $\begin{bmatrix} k_p & k_d & K & u \end{bmatrix} = \begin{bmatrix} .61 & .04 & .16 & 0 \end{bmatrix}$. This demonstrates the utility of the optimization as it finds the the base angular velocity should be zero. This corresponds to the scenario of having the agents simply spread out and then stop moving. This should be expected as there is no need for a base angular velocity to keep the agents close to a moving center. Moreover, we see that the other gains are also significantly different, showing the utility of choosing gains based on the optimization framework.

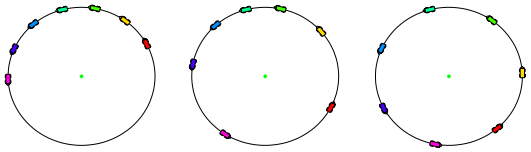

Fig. 13: This figure shows the result of having $f_c = [0 \quad 0]^T$. It shows three snapshots side by side as the agents spread out along the perimeter.

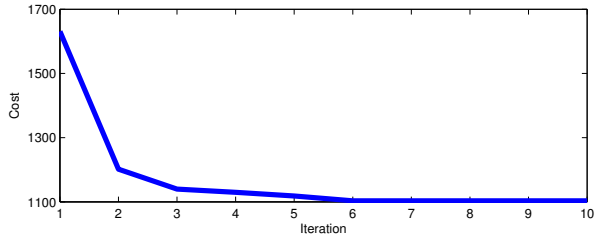

Fig. 14: This shows the cost minimization corresponding to produce the results shown in Figure 13

VI. Conclusions

In this paper, we proposed a new Kuramoto-like model for balanced deployment in multi-robot coordination tasks. Only local information of each robot's two neighbors on a cycle graph is needed for this model to spread the robots equidistantly on a circle due to its decentralized nature. We also demonstrated the application of this proposed model in a nonlinear convoy protection scenario based on parameter optimization for choosing the coupling weights. Some future works include the analysis of the convergence rate of this proposed model. We would also like to extend the circular motion to other more interesting forms of trajectories.

Acknowledgments

We would like to thank Dr. Martin Schröter, Department of Mathematics II, and Dr. Martin Lamprecht, Department of Mathematics IV, University of Würzburg, for the insightful discussions.

References

[1] X.C. Ding, A.R. Rahmani, and M. Egerstedt. Multi-UAV convoy protection: an optimal approach to path planning and coordination. *IEEE Transactions on Robotics*, 26(2):256–268, 2010.

[2] R.W. Beard, T.W. McLain, D.B. Nelson, D. Kingston, and D. Johanson. Decentralized cooperative aerial surveillance using fixed-wing miniature uavs. *Proceedings of the IEEE: Special Issue on Multi-Robot Systems*, 94(7):1306–1324, 2006.

[3] R.W. Beard, J. Lawton, and F.Y. Hadaegh. A coordination architecture for spacecraft formation control. *IEEE Transactions on Control Systems Technology*, 9(6):777–790, 2001.

[4] W. Ren and R.W. Beard. Formation feedback control for multiple spacecraft via virtual structures. In *IEEE Proceedings on Control Theory and Applications*, volume 151, pages 357–368. IET, 2004.

[5] Z. Lin, B. Francis, and M. Maggiore. Feasibility for formation stabilization of multiple unicycles. In *43rd IEEE Conference on Decision and Control, 2004. CDC.*, volume 3, pages 2447–2452. IEEE, 2005.

[6] B.S. Smith, J. Wang, M. Egerstedt, and A. Howard. Automatic formation deployment of decentralized heterogeneous multi-robot networks with limited sensing capabilities. In *IEEE International Conference on Robotics and Automation, 2009. ICRA'09.*, pages 730–735. IEEE, 2009.

[7] J. Cortes, S. Martinez, T. Karatas, and F. Bullo. Coverage control for mobile sensing networks. *IEEE Transactions on Robotics and Automation*, 20(2):243–255, 2004.

[8] M. Ji and M. Egerstedt. Observability and estimation in distributed sensor networks. In *46th IEEE Conference on Decision and Control, 2007*, pages 4221–4226. IEEE, 2007.

[9] M. Mesbahi and M. Egerstedt. *Graph Theoretic Methods in Multiagent Networks*. Princeton University Press, Princeton, NJ, Sept. 2010.

[10] Y. Kuramoto. Self-entrainment of a population of coupled non-linear oscillators. In *International symposium on mathematical problems in theoretical physics*, pages 420–422. Springer, 1975.

[11] Y. Kuramoto. *Chemical oscillations, waves, and turbulence*. Springer-Verlag (Berlin and New York), 1984.

[12] S.H. Strogatz. From kuramoto to crawford: exploring the onset of synchronization in populations of coupled oscillators. *Physica D: Nonlinear Phenomena*, 143(1):1–20, 2000.

[13] A. Jadbabaie, N. Motee, and M. Barahona. On the stability of the kuramoto model of coupled nonlinear oscillators. In *Proceedings of the American Control Conference, 2004*, volume 5, pages 4296–4301. IEEE, 2004.

[14] N. Chopra and M.W. Spong. On exponential synchronization of kuramoto oscillators. *IEEE Transactions on Automatic Control*, 54(2):353–357, 2009.

[15] F. Dörfler and F. Bullo. Synchronization and transient stability in power networks and non-uniform kuramoto oscillators. In *American Control Conference (ACC), 2010*, pages 930–937. IEEE, 2010.

[16] D.J. Klein, P. Lee, K.A. Morgansen, and T. Javidi. Integration of communication and control using discrete time kuramoto models for multivehicle coordination over broadcast networks. *IEEE Journal on Selected Areas in Communications*, 26(4):695–705, 2008.

[17] S. Susca, F. Bullo, and S. Martinez. Synchronization of beads on a ring. In *IEEE Conference on Decision and Control*, pages 4845–4850, New Orleans, LA, USA, December 2007.
[18] H.K. Khalil. *Nonlinear Systems*. Prentice Hall, Inc., Upper Saddle River, NJ, 2002.
[19] D.E. Kirk. *Optimal control theory: an introduction*. Dover Pubns, 2004.
[20] T.M. Howard. *Adaptive Model-Predictive Motion Planning for Navigation in Complex Environments*. PhD thesis, Carnegie-Mellon University, Pittsburgh, PA, 2009.
[21] G. Droge and M. Egerstedt. Behavior-based switch-time mpc for mobile robots. In *IEEE/RSJ International Conference on Intelligent Robots and Systems (IROS)*. IEEE, 2012.
[22] S. Boyd. *Convex Optimization*. Cambridge: Cambridge University Press, 2004.

APPENDIX
COSINE POSITIVE

Proposition 1: Given a set $x = \{x_1, x_2, ..., x_N\}$, where $x_i \in [0, 2\pi)$, $\sum_{i=1}^{N} x_i = 2\pi$ and $N > 2$. Then,

$$\sum_{i=1}^{N} (x_{i+1} - x_i) \cos x_i \geq 0$$

where $x_{N+1} \triangleq x_1$. The equality corresponds to the case where $x_i = \frac{2\pi}{N}, \forall i \in \{1, 2, ..., N\}$.

In order to prove this proposition, the following two Lemmas are needed.

Lemma 1: Given a set $x = \{x_1, x_2, ..., x_n\}$, where $n \in \mathbb{N}$, $x_i \in [0, 2\pi)$, $\sum_{i=1}^{n} x_i = 2\pi$ and $n > 2$. Then, $\forall k, l \in \{1, 2, ..., n\}$, we have $x_k \leq x_l$ iff. $\cos x_k \geq \cos x_l$.

Proof: We first show that if $x_k \leq x_l$, then $\cos x_k \geq \cos x_l$ in the following two cases:

- $x_k \leq x_l < \pi$: The monotonicity of cosine function clearly implies $\cos x_k \geq \cos x_l$.
- $\pi \leq x_l$: Consider the following inequality:

$$0 < x_k = 2\pi - \sum_{j=1, j\neq k}^{n} x_j \leq 2\pi - x_l \leq \pi.$$

Hence, in this case,

$$\cos x_k \geq \cos(2\pi - x_l) = \cos x_l.$$

Now we will show if $\cos x_k \geq \cos x_l$, then $x_k \leq x_l$ by contradiction. Suppose we have $\cos x_k \geq \cos x_l$ and $x_k > x_l$. From the analysis above, $x_k > x_l$ implies $\cos x_k < \cos x_l$, which is a contradiction to the assumption. This completes the proof. ∎

Now we will present a stronger form of Proposition 1 in the following Lemma.

Lemma 2: Suppose that a set $x = \{x_1, x_2, ..., x_n\}$, where $n \in \mathbb{N}$ and $x_i \in [0, 2\pi)$, is such that $\forall k, l \in \{1, 2, ..., n\}$, $x_k \leq x_l$ iff. $\cos x_k \geq \cos x_l$. Then,

$$f_n(x) \triangleq \sum_{i=1}^{n} (x_{i+1} - x_i) \cos x_i \geq 0, \tag{31}$$

where $x_{n+1} \triangleq x_1$.

Proof: We can prove this by induction to n.

- $n = 1$: The proof is trivial.
- $n = 2$: W.l.o.g., we can assume $x_2 \geq x_1$, and therefore, $\cos x_2 \leq \cos x_1$. With these two inequalities, it implies:

$$\begin{aligned} f_n(x) &= (x_2 - x_1)\cos x_1 + (x_1 - x_2)\cos x_2 \\ &\geq (x_2 - x_1)\cos x_2 + (x_1 - x_2)\cos x_2 \\ &= 0. \end{aligned}$$

- $n > 2$: There must be a $j \in \{1, 2, ..., n\}$ s.t. $x_{j-1} \leq x_j$ and $x_{j+1} \leq x_j$. Because, otherwise we would have:

$$x_1 \leq x_2 \leq \cdots \leq x_n \leq x_{n+1} = x_1,$$

or

$$x_1 \geq x_2 \geq \cdots \geq x_n \geq x_{n+1} = x_1,$$

which would imply that all x_i are equal (thus the proof is trivial). Now for such a j, we have $\cos x_{j-1} \geq \cos x_j$ and $\cos x_{j+1} \geq \cos x_j$. Therefore,

$$\begin{aligned} f_n(x) &= \sum_{i=1}^{n} (x_{i+1} - x_i)\cos x_i \\ &= (x_j - x_{j-1})\cos x_{j-1} + (x_{j+1} - x_j)\cos x_j \\ &\quad + \sum_{\substack{i=1 \\ i\neq j-1, j}}^{n} (x_{i+1} - x_i)\cos x_i \\ &= (x_j - x_{j+1})\cos x_{j-1} + (x_{j+1} - x_{j-1})\cos x_{j-1} \\ &\quad + (x_{j+1} - x_j)\cos x_j \\ &\quad + \sum_{\substack{i=1 \\ i\neq j-1, j}}^{n} (x_{i+1} - x_i)\cos x_i \\ &\geq (x_{j+1} - x_{j-1})\cos x_{j-1} \\ &\quad + \sum_{\substack{i=1 \\ i\neq j-1, j}}^{n} (x_{i+1} - x_i)\cos x_i \end{aligned}$$

The last expression has the form of $f_{n-1}(x)$ (It has $n-1$ terms, without the contribution from x_j, not x_n), which implies that $f_n(x) \geq f_{n-1}(x)$. And by the induction hypothesis, $f_n(x) \geq 0$. The equality only holds when $x_j = x_{j-1}, \forall j \in \{1, 2, ..., N\}$. Considering the condition that $\sum_{i=1}^{n} x_i = 2\pi$, the equality indicates $x_i = \frac{2\pi}{N}$.

This completes the proof of the Lemma. ∎

From Lemma 1 and 2, we can conclude that Proposition 1 is proved.